Available online at www.sciencedirect.com

Chemical Engineering Research and Design

journal homepage: www.elsevier.com/locate/cherd

Bio-inspired membranes for adsorption of arsenic via immobilized L-Cysteine in highly hydrophilic electrospun nanofibers

David Picón[a,b], Nicolás Torasso[a,b], José Roberto Vega Baudrit[c,d], Silvina Cerveny[e,f,*], Silvia Goyanes[a,b,**]

[a] Universidad de Buenos Aires, Facultad de Ciencias Exactas y Naturales, Departamento de Física (C1428EGA), Buenos Aires, Argentina

[b] CONICET - Universidad de Buenos Aires, Instituto de Física de Buenos Aires - CONICET (IFIBA) (C1428EGA), Buenos Aires, Argentina

[c] National Laboratory of Nanotechnology, National Center of High Technology (LANOTEC-CeNAT-CONARE), 1174-1200 Pavas, San José, Costa Rica

[d] Laboratory of Polymers (POLIUNA), National University of Costa Rica (UNA), Heredia 86-3000, Costa Rica

[e] Centro de Física de Materiales (CSIC, UPV/EHU)-Materials Physics Center (MPC), Paseo Manuel de Lardizabal 5, San Sebastián 20018, Spain

[f] Donostia International Physics Center (DIPC), San Sebastián 20018, Spain

ARTICLE INFO

Article history:
Received 5 May 2022
Received in revised form 22 June 2022
Accepted 27 June 2022
Available online 30 June 2022

Keywords:
Arsenic adsorption
PVA membranes
Electrospun nanofibers
L-Cysteine

ABSTRACT

Arsenic is a concern for its ubiquity in the environment and its accumulative and toxic properties. Water is often contaminated with this chemical, so developing simple, scalable, and green water treatment technologies is urgently needed. We show here that the ability of the L-Cysteine biomolecule to form complexes with arsenic inspires its use as a natural bio-inspired sorbent to develop advanced functional materials. We establish for the first time a way to chemically anchor L-Cysteine (L-Cys) inside highly hydrophilic nanofibers to create a membrane capable of lowering As(V) concentration below the WHO limit of 10 µg/L. A homogeneous precursor mixture of an aqueous solution of PVA and L-Cys (5 wt% and 10 wt% of L-Cys with respect to PVA) was electrospun to obtain a nanofibrous membrane. Successful immobilization of L-Cys within PVA nanofibers is achieved during heat treatment at 190 °C. It occurs through esterification reactions between the hydroxyl group on the PVA chain and the carboxylic acid on L-Cys. Arsenic sorption (as As (V)) was assessed by batch experiments in aqueous media and at a controlled pH range. The maximum removal efficiency was achieved at pH 7, supporting the formation of thiolate complexes as the primary mechanism for arsenic sorption. We show that L-Cys confinement makes arsenic diffusion inside the nanofibers a rate-limiting process in adsorption kinetics, following the pseudo first order equation. Overall, this work establishes a novel arsenic remediation strategy and encourages the research of nature-

* Corresponding author at: Centro de Física de Materiales (CSIC, UPV/EHU)-Materials Physics Center (MPC), Paseo Manuel de Lardizabal 5, San Sebastián 20018, Spain.

** Corresponding author at: Universidad de Buenos Aires, Facultad de Ciencias Exactas y Naturales, Departamento de Física (C1428EGA), Buenos Aires, Argentina.

E-mail addresses: scerveny@ctq.csic.es, silvina.cerveny@ehu.es (S. Cerveny), sgoyanes@gmail.com (S. Goyanes).

https://doi.org/10.1016/j.cherd.2022.06.042

0263-8762/© 2022 The Author(s). Published by Elsevier Ltd on behalf of Institution of Chemical Engineers. CC_BY_NC_ND_4.0

mimicking adsorbents and biodegradable polymers to develop functional materials in water remediation.

© 2022 The Author(s). Published by Elsevier Ltd on behalf of Institution of Chemical Engineers.
CC_BY_NC_ND_4.0

1. Introduction

While arsenic (As) is considered one of the most dangerous hazards in drinking water, at least 140 million people in fifty countries are exposed to high levels of As, beyond the current WHO guideline value (10 μg/L) (Litter et al., 2019; WHO, 2017). In Argentina, 4 million people live in areas contaminated with arsenic, reaching up to 2000 μg/L in some regions (CONICET, 2018) and, due to geological and environmental conditions, the main arsenic species present in human consumption waters is As(V) (Litter et al., 2019; CONICET, 2018). Long-term consumption of As contaminated water may lead to severe diseases such as skin lesions, hyperkeratosis, bladder or lung cancer (Mohammed Abdul et al., 2015). In particular, the toxicity of inorganic arsenic species, the main species found in water, likely occurs either by replacing phosphate anion in some metabolic processes or by binding with sulfhydryl groups (R-SH) in proteins (Shen et al., 2013; Tam et al., 2020).

Recently, bio-based sorbents have shown to be a promising approach for environmental remediation, including arsenic. They are eco-friendly, sustainable, cost-effective, and have a similar performance to traditional adsorbents (Giri et al., 2021; Solangi et al., 2021). Due to its unique chemical properties, the biomolecule L-Cysteine (L-Cys) can be used to develop materials with the ability to form complexes with arsenic and remove this metalloid from water. L-Cys (Fig. 1) is a semi-essential amino acid containing an R-SH group with crucial functions in various biological processes. It is frequently detected in functional sites of proteins even though it is not an amino acid often observed in proteins and enzymes. Due to its reactivity, redox activity, polarizability, and high binding affinity for metals (such as arsenic (Poole, 2015; Shen et al., 2013; Timalsina et al., 2021)), L-Cys is an excellent candidate for incorporating adsorbents for this specific metal. The reaction between arsenic and sulfhydryl (thiol) compounds involves displacing the -OH ligands in the arsenic species by the R-SH group to yield the corresponding thiolate complexes (Carrero et al., 2001; Spuches et al., 2005).

Several works have reported the use of the thiol group for environmental remediation. For example, thiol-functionalized chitin nanofibers for As(III) adsorption were prepared by grafting L-Cys on the chitin surface (Yang et al., 2015). Chen et al. (2019). prepared nanoscale dialdehyde cellulose–cysteine fibers to remove As(III) from the water showing high adsorption capacity. Also, keratin protein has been used to improve arsenic removal efficiency, given that it contains around 20% by weight of L-Cys (Timalsina et al., 2021). L-Cys-based surfactants have also been synthesized as an environmentally friendly and biodegradable material with a cysteine headgroup for selective As(V) binding in water treatment (Makavipour et al., 2019). The surface functionalization of magnetic nano-magnetite nanoparticles with L-Cys (Fe_3O_4@Cy) presented improved stability and enhanced arsenite and arsenate adsorption efficiency (Tripathy et al., 2020). The arsenic removal efficiency in these previous works ranged from 27% to 75%, and the adsorption process required long contact times. In most cases, the adsorption experiments were conducted at initial arsenic concentrations ranging from 5 mg/L to 2500 mg/L, far above the typical levels found in drinking water. Furthermore, one drawback of using loose adsorbents is that removing them requires an extra process, often adding another filtering step. Without immobilizing them inside a membrane, the adsorbent might be released into the water with further contamination of the environment.

A great way to immobilize thiol groups could be achieved by anchoring them in a permeable, self-standing membrane capable of interchanging water with the medium. In fact, incorporating adsorbents within a membrane has shown to be an effective way to remove arsenic from water (Zhang et al., 2021). In this sense, electrospinning is a versatile and scalable approach to producing porous membranes with high permeability and a great surface area made up of nano or sub-micron polymeric fibers. Electrospun membranes are a complex and advanced functional structure with unique properties compared to other bio-sorbents such as films or gels. For example, electrospun nanofibers have a tunable porous structure that allows their use as microfiltration membranes (Gonçalves et al., 2022). These fibers may contain additives or be functionalized for specific purposes like water remediation, air filtration, adsorption, catalysis, etc. (Ray et al., 2016; Ribba et al., 2017). Among available electrospinning polymers, poly (vinyl alcohol) (PVA) is soluble in water, bio-compatible, and non-toxic. It also has good thermal and chemical stability (Koski et al., 2004). The insolubility of an electrospun PVA membrane can be achieved with a proper heat treatment or crosslinking agent (López-Córdoba et al., 2016; Estevez-Areco et al., 2018). In particular, insoluble electrospun PVA has been successfully applied as a membrane for the filtration of TiO_2 NPs and as high-flux microfiltration filters (Cimadoro and Goyanes, 2020; Liu et al., 2013).

Moreover, the fibers swell underwater because they are still hydrophilic after insolubilization (Cimadoro and Goyanes, 2020; Miraftab et al., 2015). PVA electrospun membranes have shown excellent performance in water remediation. For example, Pereira et al. (2021) reported a novel bio-hybrid membrane of PVA nanofibers and free-living bacteria to simultaneously remove Cr(VI) and phenol. Likewise, PVA nanofibers crosslinked with glutaraldehyde were capable of absorbing Pb(II) and Cu(II) (Tian et al., 2019). In particular, for arsenic removal, high As(V) adsorption was achieved by confining and dispersing iron oxide nanoparticles inside electrospun PVA nanofibers (Torasso et al., 2020). Other functionalized electrospun membranes have been reported to remove arsenic from water using chitosan, an amino-based biopolymer (Talukder et al., 2021; Min et al., 2019), or styrene–divinylbenzene copolymer functionalized with phosphonium pendant groups impregnated with crown ether and iron ions showing high adsorption in the 25–175 μg/L range (Negrea et al., 2014). Although, in the literature is reported that electrospun nanofibers are modified

Table 1 – Composition and properties of electrospun solutions. Conductivity and viscosity were measured at 25 °C. Suffix HT in sample names stands for heat-treated membranes.

Sample	% PVA (w/w)	% CA (w/w)[a]	% L-Cys (w/w)[a]	Conductivity (mS/cm)	Viscosity (cP)
PVA	11	10	–	0.91 ± 0.01	380 ± 3
PVA-LCys 5%	11	10	5.0	3.97 ± 0.01	347 ± 3
PVA-LCys 10%	11	10	10	8.31 ± 0.01	348 ± 3

[a] Percentage respect to the mass of PVA in solution (wt%/PVA weight).

to incorporate L-Cys, such functionalization is performed in additional steps that require the use of chemicals harmful to the environment. Thus, the final product is made of metallic oxides nanofibers for sensing purposes (Arvand and Sayyar Ardaki, 2017; Halicka and Cabaj, 2021; Oliveira et al., 2020). There are no reports of in situ incorporation of the amino acid into electrospun PVA membranes for remediation, particularly for arsenic removal.

Here we developed a novel electrospun PVA membrane containing immobilized L-Cys, preventing the migration of the sorbent to the environment, and assessed its efficiency for the removal of arsenic from water. The specific objectives are (i) use a green process via electrospinning of an aqueous solution of PVA and L-Cys followed by heat treatment at 190 °C to produce a self-supporting membrane, that is insoluble in water, (ii) reach the removal of arsenic to 10 µg/L, the maximum permitted by WHO, and (iii) perform the removal at pH 7, the optimal for a drinking water treatment in a short contact time. We show, via thermal and structural characterizations, that heat treatment (never used in the literature for these membranes) is a fundamental step for covalently attaching L-Cys to PVA chains through an esterification reaction. Batch experiments at different pH values evaluated the As(V) removal performance of the membrane. These results indicate that the thiol group is mainly responsible for As(V) capturing through a complexation reaction. Finally, kinetic experiments suggest that the encapsulation of L-Cys makes diffusion of arsenic species inside the nanofibers a rate-limiting step for adsorption. All experiments were done at typical concentrations commonly detected in Buenos Aires province, Argentina.

2. Materials and methods

2.1. Materials

PVA (Mowiol 10–98) with MW = 61,000 g/mol and 98% degree of hydrolysis was supplied from Sigma Aldrich. Citric acid (CA), L-Cysteine hydrochloride (L-Cys), ascorbic acid, antimonyl tartrate, and ammonium molybdate were purchased from Biopack (Argentina). All these chemicals were 98% pure or higher. Sulfuric acid (98% wt.) and hydrochloric acid (36% wt.) were supplied by Cicarelli (Argentina). A 1000 mg/L $NaH_2AsO_4{\cdot}7H_2O$ standard solution (Merck) was used in arsenic adsorption experiments. Deionized water was used to prepare reagents and stock solutions.

2.2. Membrane preparation

PVA and citric acid (CA) were dissolved in water at 80 °C for 2 h under stirring to obtain a homogeneous mixture. After cooling to room temperature, L-Cys was added and stirred for 24 h. Table 1 describes each sample's electrospinning solution and nomenclature. These solutions were electrospun using an electrospinning machine (Tong Li Tech, China) at 30 kV, an injection rate of 0.5 mL/h per needle, and a collector distance of 12.5 cm. The membranes were heat-treated (HT) at 190 °C for 10 min to obtain a water-insoluble material (Cimadoro and Goyanes, 2020). Solution viscosity and conductivity were measured with a Brookfield viscometer (model LV-DV-E) and an Orion Versastar conductometer (Thermo scientific).

To study the possible loss of L-Cys during membrane contact with water, samples of heat-treated membranes (2 × 2 cm^2) were immersed in water at room temperature (22–25 °C) for 24 h under orbital shaking at 120 rpm. Then, the samples were dried at 50 °C until constant weight (Cimadoro and Goyanes, 2020) and characterized by SEM, FTIR, and TGA.

2.3. Adsorption experiments

Batch experiments were carried out at a fixed amount of bio-adsorbent (670 mg/L of L-Cys) and 300 µg/L As(V) initial concentration, at room temperature in a rotary shaker at 120 rpm to determine the material performance for arsenic removal. Batch experiments are the standard procedure to test the adsorption capacity and kinetics of materials, including bio-sorbents and electrospun membranes like the one presented in this study (Bahmani et al., 2019; Guo et al., 2021; Min et al., 2015). Optimal pH for arsenic adsorption was tested by measuring equilibrium concentrations (24 h) for a 100 µg/L As(V) in the pH range from 4 to 10, fixed either using a citrate buffer (up to pH 7) or a 0.1 M NaOH solution (from pH 8 to 10). The As concentration used in pH studies was similar to that found in 60% of the districts studied in Buenos Aires province, Argentina (Bardach et al., 2015; Litter et al., 2019). For kinetic studies, pH was adjusted to 7 with a citrate buffer, and arsenic concentration was measured at times between 15 min and 24 h.

The removal efficiency (%R) was calculated as

$$\%R = (Ci - Cf) / (Ci)\ 100\%$$

where *Ci* and *Cf* are the initial and equilibrium As(V) concentrations respectively. As(V) concentration was measured according to a well-known arsenomolybdate colorimetric method (Baigorria et al., 2020; Dhar et al., 2004) using an UV spectrophotometer (Shimadzu UV-Vis 1800), with little modification in the mixing ratio of the reagent for the color development. The optimal mixing ratio was found to be 2:3:1.5:6 for the solutions of ascorbic acid, ammonium molybdate solution, potassium antimonyl tartrate and sulfuric acid respectively. This colorimetric method has proven to be simple, economical, and suitable to study the arsenic removal efficiency of polymeric nanocomposites (Baigorria et al., 2020). The calibration solutions and blanks were prepared with a citrate buffer to consider possible interference in the methodology. To dismiss possible reduction of As(V) to

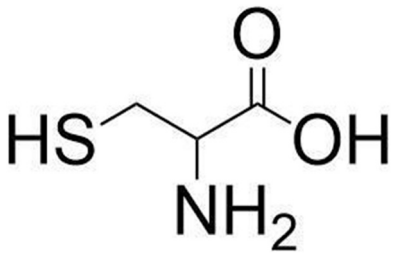

Fig. 1 – Molecular structure of L-Cysteine, a thiol-containing amino acid.

As(III) by L-Cysteine, a 2 mM KIO_3 oxidizing solution was added to the samples before analysis (Dhar et al., 2004).

All adsorption experiments were performed in triplicate. The error was estimated as the standard deviation of the three measurements. The quantification limit of the spectrophotometric method was 10 µg/L.

2.4. *Characterizations*

Chemical characterization was performed by ATR-FTIR (model 4100, Jasco, Japan). Spectra were recorded from 4000 cm^{-1} to 600 cm^{-1} with a resolution of 4 cm^{-1}. The C-H bending (-CH_2) at 1421 cm^{-1} was selected as the reference band, given that it was not expected to change after the ester/crosslink reaction (López-Córdoba et al., 2016). The intensity ratio of the band of interest to the reference band was calculated to track relative changes in the functional groups of the samples.

Morphology of the membranes was observed by SEM using a JEOL JSM 6390LV operated at 30 kV. Elemental composition was evaluated by EDX. Contact angle was studied using an Optical Tensiometer (OneAttension theta – Biolin Scientific). Thermogravimetric analysis (TG) and differential thermal analysis (DTA) were performed in a Shimadzu DTG-60 (Japan) under a dry nitrogen atmosphere in the range of 25–550 °C at a heating rate of 10 K/min. Differential scanning calorimetry (DSC) measurements were performed on ~10 mg samples using a TA Instruments Q2000 at a heat rate of 5 K/min. The samples were placed in non-hermetic aluminum pans and put through a previous drying sequence up to 150 °C. A helium flow rate of 25 mL/min was used at all times. Glass transition of the materials (T_g) was obtained using the bisector method.

3. Results and discussion

3.1. *Surface morphology analysis*

The developed PVA-LCys membranes are homogeneous and self-supporting, and their thickness can be controlled by the electrospinning time (see Fig. S0). Their morphology and composition are essential aspects that determine their functionality as an adsorbent for arsenic. Thus, the nanofiber structure was first analyzed via scanning electron microscopy, shown in Fig. 2. The typical porous structure of randomly oriented nanofibers produced by electrospinning with nanofiber diameters of (120 ± 10) nm can be seen. Adding L-Cys increases the rugosity of the fibers and the diameter distribution width without significantly changing the mean of the nanofiber diameters. EDX analysis confirms the presence of L-Cys through sulfur detection and shows that the sulfur content of PVA-LCys 10% HT doubles that of PVA-LCys 5% HT.

3.2. *FTIR analysis*

In Fig. 3, a comparison of the FTIR spectra of samples before and after heat treatment is shown. It is seen that the anchoring of the L-Cys to the PVA chain is performed during the heat treatment through the reaction between the -OH group in the PVA and the -COOH group of the L-Cys. Also, it is observed that the L-Cys remain covalently attached to the nanofibers after washing (Fig. 3(b)).

The presence of L-Cys within the PVA nanofibers is also revealed in the FTIR spectra through the presence of amino group bands. The asymmetric bending vibration of the -NH_2 group at 1619 cm^{-1} (Kogelheide et al., 2016; Pereira et al., 2014)

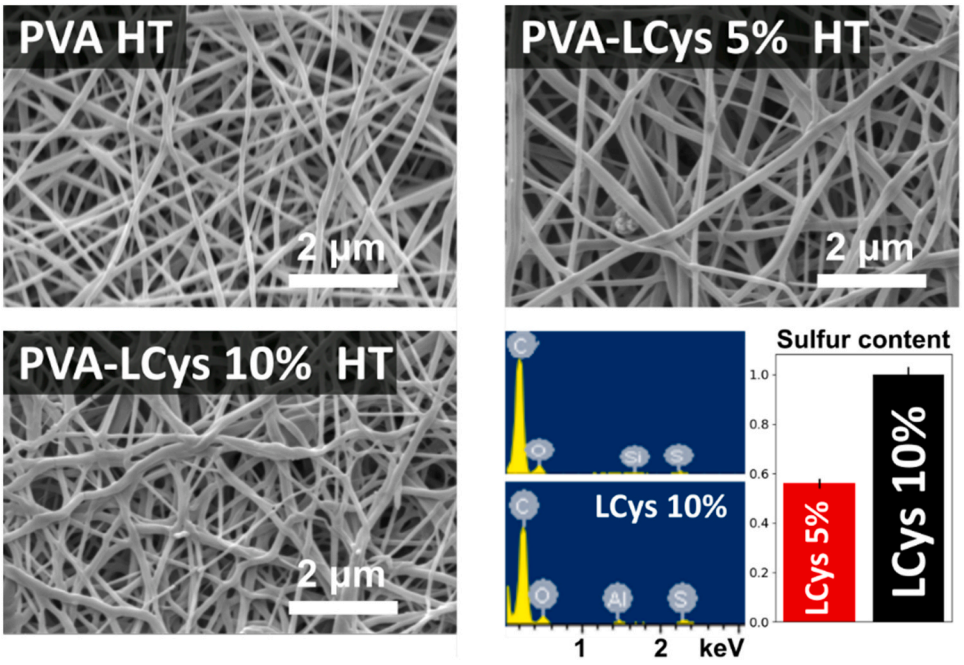

Fig. 2 – SEM images of PVA and PVA-LCys heat-treated samples. EDS spectra of PVA-LCys 5% HT and PVA-LCys 10% HT are also shown, along with the corresponding relative sulfur content.

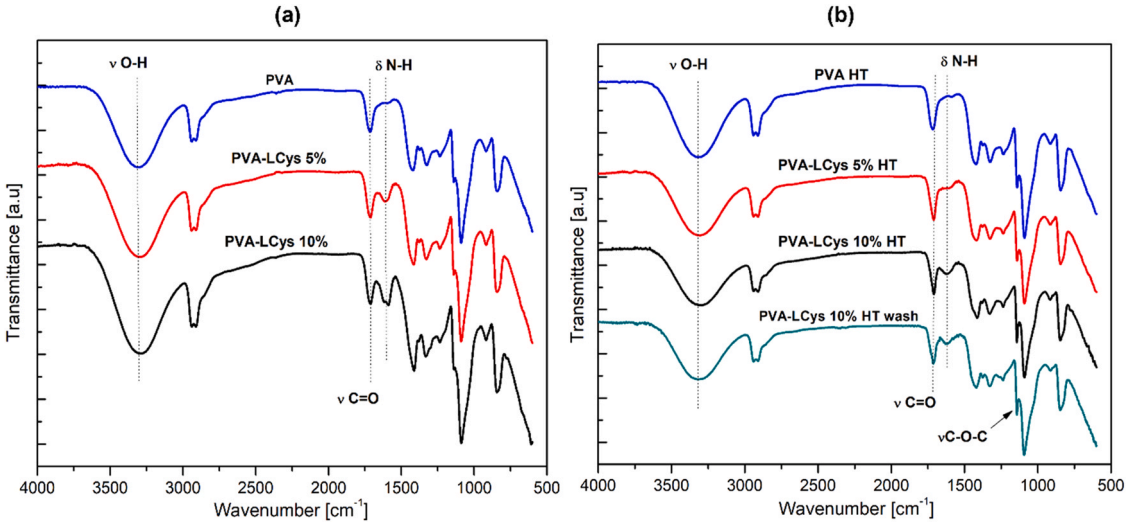

Fig. 3 – FTIR spectra of samples (a) before heat treatment, and (b) after heat treatment and after washing.

is observed in the samples before and after heat treatment, and even after washing (Fig. 3(a) and (b) respectively).

All spectra showed the characteristic PVA absorption bands: C-H symmetric (2910 cm^{-1}) and asymmetric (2939 cm^{-1}) stretching, C-H bending at 1421 cm^{-1}, O-H bending at 1328 cm^{-1}, C-O stretching at 1089 cm^{-1}, C═O stretching at 1716 cm^{-1} and O-H stretching at 3314 cm^{-1} (Estevez-Areco et al., 2018; Vergara-Rubio et al., 2022). Some PVA bands are also present in the PVA-LCys spectrum, and, as can be seen in Table S1 (in Supplementary information), their relative intensity increases with the content of L-Cys in the materials.

By comparing Fig. 3(a) and (b), it is observed that heat treatment changes the chemical structure of PVA and PVA-LCys membranes. The main difference between the treated (Fig. 3(b)) and the untreated samples (Fig. 3(a)) is the increase of the peak at 1142 cm^{-1} assigned to C-O-C stretching (Socrates, 2004). Besides, the O-H bending and stretching vibrations are less intense in PVA-LCys HT than in the PVA-LCys spectrum.

Note that all samples were prepared with CA and that PVA can undergo esterification/crosslinking reaction with either CA or L-Cys (López-Córdoba et al., 2016). Hence, in PVA HT spectra, the C═O and C-O-C bands are assigned to ester/crosslinking reactions between PVA and CA. Furthermore, the relative intensity of C-O-C increases with L-Cys content (I_{1142}/I_{1421} ratio in Table S1 in SI), which is probably due to further esterification reactions between the -OH group in PVA and the -COOH group in L-Cys. This fact is also supported by less intense O-H bending and stretching vibrations in PVA-LCys HT compared to the PVA HT spectrum (I_{3314} / I_{1421} in Table S1 in SI). The extent of the esterification reaction significantly increases with L-Cys content, which can be estimated by the intensity ratio of C═O to O-H bands (I_{1716}/I_{3314}) (Sonker et al., 2018). Given that the content of CA is the same for every sample, these results provide clear evidence of the PVA chain´s functionalization with L-Cys through an esterification reaction during heat treatment.

L-Cys immobilization within PVA nanofibers through covalent bonding prevents them from leaching into the water when submerged for arsenic adsorption. This hypothesis is confirmed, given that the FTIR spectrum of PVA-LCys 10% HT wash sample (Fig. 3(b)) does not present differences from that of PVA-LCys 10% HT.

3.3. *Thermal degradation*

Thermogravimetric analysis can also assess L-Cys content and interaction with the membrane. TG measurements were performed on bulk L-Cys, on the membranes before and after heat treatment (see Fig. 4(a) and (b)), and on washed PVA-LCys 10% HT (Fig. 4(c)).

Fig. 4(a) shows that bulk L-Cys abruptly degrades and loses 74% of its mass at 250 °C. In PVA-LCys samples, this would represent a 3.7 and 7.4 wt% loss for PVA-LCys 5% and PVA-LCys 10% membranes, respectively. Effectively, the inset of Fig. 4(a) shows an increased weight loss at 250 °C for samples containing L-Cys: 3.3% for PVA-LCys 5% and 6.4% for PVA-LCys 10%. These results suggest that L-Cys content is roughly two times higher in PVA-LCys 10% than PVA-LCys 5% sample. This tendency was also observed in the -NH_2 band ratio in FTIR studies (see I_{1619}/I_{1421} in Table S1 in SI) and in EDS analysis.

Three clear degradation steps can be observed for the membranes, corresponding to evaporation of adsorbed water (up to 100 °C), degradation of side groups (300–400 °C) which form water and other volatile compounds such as ketones and acetaldehyde, and decomposition of the main polymer chain (400–450 °C) (de Dicastillo et al., 2017; Holland and Hay, 2001). Fig. 4(b) shows that adding L-Cys scarcely increases the thermal stability of the heat-treated membranes, delaying the beginning of the side group's degradation (the peak shifts towards higher temperatures by only 3 °C (see also DTG curves in Fig. 5)). This behavior was also reported by Sonker et al. (2018) for PVA films crosslinked with suberic or terephthalic acid, in which the decomposition temperature increased with the concentration of organic acid. L-Cys degradation is not seen in TGA degradation curves of heat-treated membranes in Fig. 4(b), suggesting that L-Cys is not free inside the nanofibers. The reduction of -OH groups in the side chains of PVA would also explain the slight increase in thermal stability for samples containing L-Cys (see also Fig. 7). Overall, these results further support the esterification reaction previously observed in FTIR studies.

It is essential to notice no significant differences in degradation curves for samples before and after washing with water (Fig. 4(c)). In particular, this means that the washing of the sample does not alter its weight loss in the L-Cys

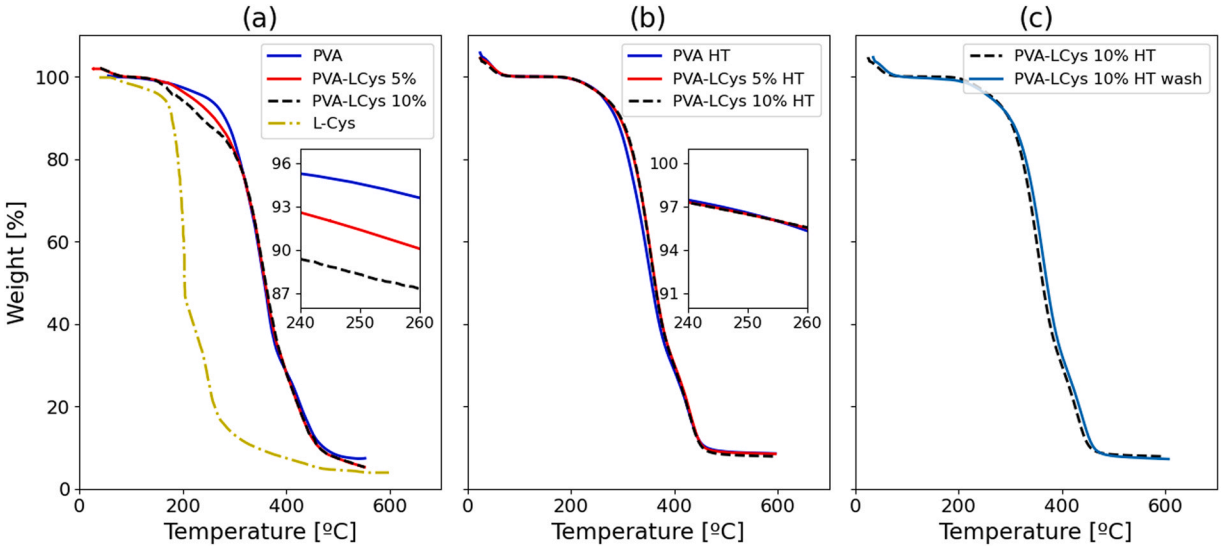

Fig. 4 – TGA analysis of the samples (a) before heat treatment, (b) after heat treatment and (c) after washing. L-Cys degradation is shown in (a). Insets show a close up on bulk L-Cys main degradation temperature.

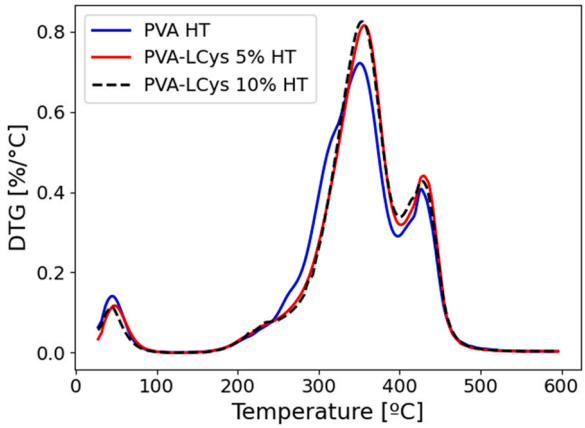

Fig. 5 – DTG of the samples with thermal treatment. Inset shows degradation of remnant un-bonded L-Cys in the samples.

degradation region, indicating that L-Cys is not lost during washing, as previously shown in FTIR studies.

3.4. *DSC analysis*

To reveal the role of L-Cys in the polymeric matrix, DSC studies of the membranes (Fig. 6) before (a) and after (b) heat treatment were performed for different contents of L-Cys. DSC curves of membranes before heat treatment show that the increase of L-Cys from 0% to 10% modifies both the amorphous and crystalline regions of the nanofibers. A systematic decrease in the glass transition temperature (77 °C, 75 °C, and 73 °C increasing the L-Cys content from 0% to 10%) suggests that L-Cys acts as a plasticizer. Furthermore, changes in the molecular interactions induced by L-Cys also affect the endothermic peak (i.e., the melting process), broadening and shifting towards higher temperatures. In particular, the broadening of the endothermic peak was reported in previous studies in which plasticizers were added to the polymeric matrix (Lim and Wan, 2008; Srithep and Pholharn, 2017).

In the case of heat-treated membranes, a new T_g arises around 125 °C. The presence of two glass transitions even for the membrane without L-Cys indicates a heterogeneous material at a microscopic level (inset of Fig. 6(b)). Some of these regions correspond to those generated by esterification/crosslink with CA, which gives a higher T_g. The other region is the unaltered polymer with a T_g around 60 °C.

Conversely, a single T_g at 125 °C is observed for L-Cys-containing membranes, possibly due to further esterification reactions involving L-Cys previously observed in FTIR studies. Interestingly, the heat treatment induces esterification of PVA with L-Cys or CA, preventing them from acting as plasticizers. These interactions also generate substantial modifications in the endothermic peak related to polymer melting. In the heat-treated materials, these peaks become sharper and shift towards higher temperatures. The broad shoulder at 150 °C vanishes, indicating a different melting process in these samples compared to membranes without L-Cys or CA. These results suggest that the plasticizers (CA and/or L-Cys) are no longer available within the structure and are now bonded with the polymer chains, according to the observations in FTIR and TGA studies.

3.5. *Water contact angle measurements*

The previously mentioned changes in membrane structure after heat treatment produce changes in their surface energy, as demonstrated by water contact angle measurements (Table 2). While the untreated membrane (PVA) immediately dissolves in water preventing contact angle measurement, the heat-treated membranes are insoluble in water. The addition of L-Cys increases water contact angle and reduces solubility in water, evidencing the increase in the number of esterification reactions. These reactions lower the surface energy of the membranes and lead to a reduction in intermolecular interaction with water.

The conjunct interpretation of FTIR, EDS, DSC, and contact angle results, indicates that the L-Cys is covalently bonded with PVA polymer chains in the nanofibers, preventing its loss by migration out of the membrane and into the water. Furthermore, the mechanism proposed for this

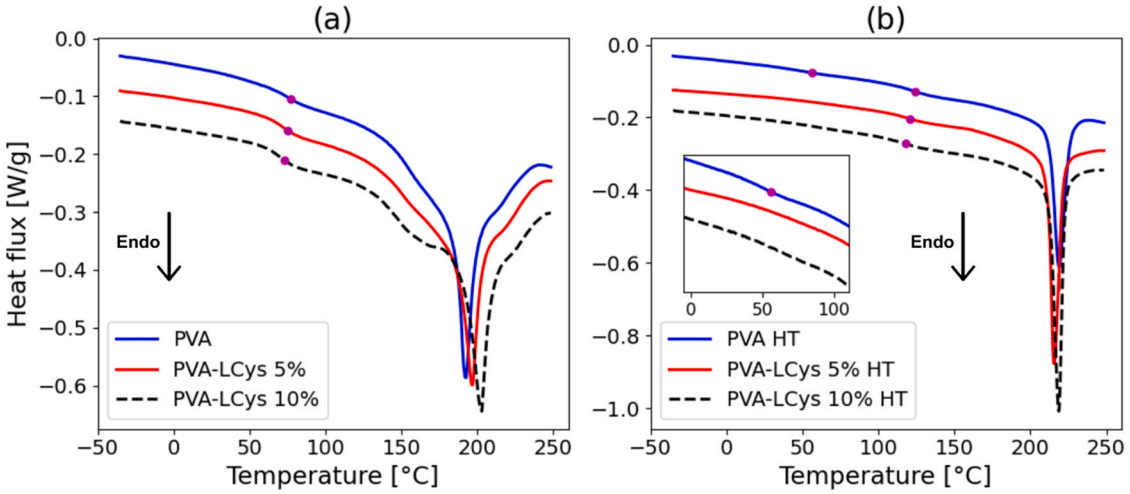

Fig. 6 – DSC analysis of PVA-L-Cys membranes before (a) and after (b) heat treatment. Purple dot indicates T_g for each material. Curves were vertically shifted for better visualization. Inset in (b) is a zoom in the low T_g region.

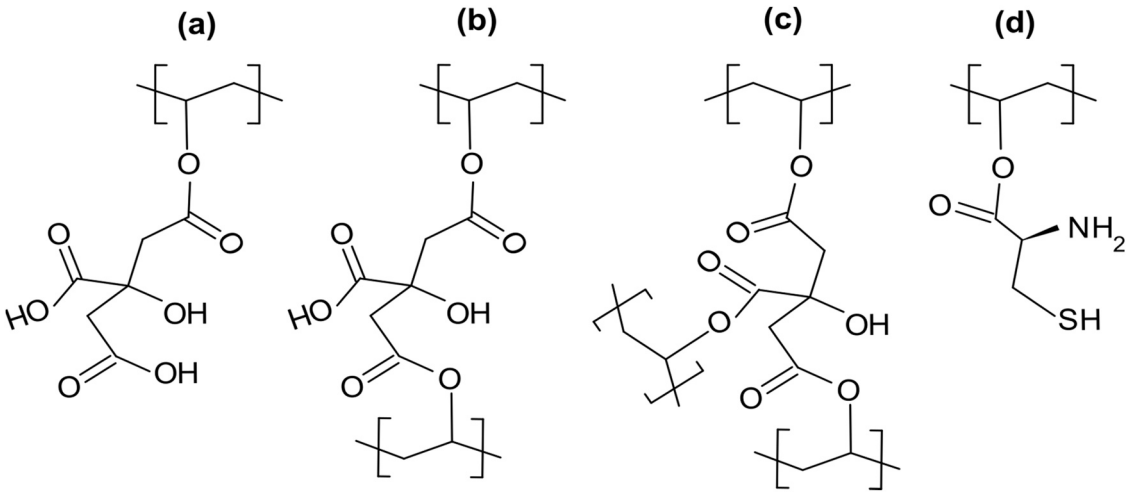

Fig. 7 – Possible reactions of CA and L-Cys with PVA chains during heat treatment of the membranes. (a) Single esterification with CA. (b, c) Double and triple esterification with CA leading to polymer crosslinking. (d) Esterification with L-Cys.

Table 2 – Contact angle and solubility in water for samples containing different amounts of L-Cys.

Material	PVA	PVA HT	PVA-LCys 5% HT	PVA-LCys 10% HT
Contact angle	Not detected	(35 ± 3)°	(67 ± 5)°	(71 ± 5)°
Drop picture	–			
Water solubility	100%	(5.5 ± 0.1) %	(1.8 ± 0.1) %	(1.7 ± 0.1) %

interaction does not affect the availability of thiol groups, responsible for arsenic adsorption.

Every study presented here showed that L-Cys content is more significant in the sample PVA-LCys 10% HT. Since arsenic adsorption occurs in thiol and/or amino groups, we chose this sample to perform arsenic adsorption experiments.

3.6. *Removal of As (V)*

3.6.1. *Effect of pH*

Arsenic contaminated groundwater is usually under neutral to slightly alkaline pH conditions (Kumar et al., 2019). In addition, the arsenic adsorbent´s performance is pH-dependent

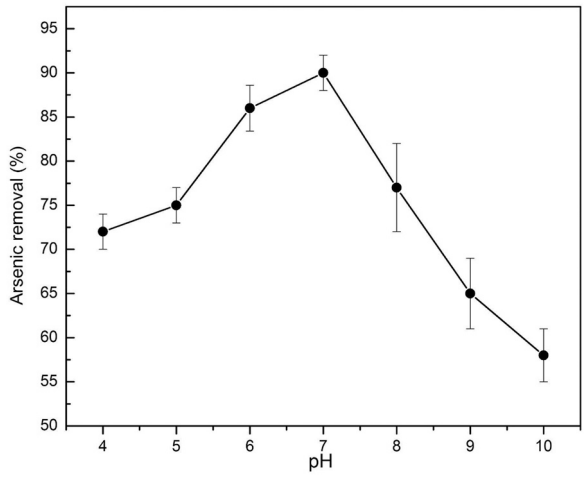

Fig. 8 – Effect of pH on the adsorption of As(V) by PVA-LCys 10% HT membrane. Initial As(V) concentration was 100 µg/L, dose of 670 mg L-Cys/L, and 24 h contact time.

(Yang et al., 2015). Therefore, it is crucial to study the removal efficiency of the PVA-LCys 10% HT membranes at different pH values. Moreover, the pH of the water determines the arsenic speciation. Fig. 8 shows the arsenic removal efficiency of the PVA-LCys 10% HT membrane at different pH values.

The maximum removal efficiency was achieved at neutral pH, which is desirable because most natural water sources have a pH near 7.

The remaining As(V) concentration after adsorption (10 µg/L) lies in the maximum permissible level of arsenic in drinking water, according to WHO (2017). This value could be even lower, considering that 10 µg/L is the limit of quantification of our method. Furthermore, this result shows that PVA-LCys 10% HT membranes are effective even in waters with low arsenic levels (< 100 µg/L), which, for example, have been reported in 290 localities of the Buenos Aires province along with the south of Santa Fe province and the Atlantic coast (Bardach et al., 2015; Litter et al., 2019; Taylor, 2017). This low-level arsenic adsorption performance surpasses previous works that use L-Cys containing adsorbents for As (V) (Makavipour et al., 2019).

The behavior observed in the removal efficiency dependence with pH (Fig. 8) owes to the formation of the well-known thiolate complex between arsenic species and L-Cys (Spuches et al., 2005), which are favored in a neutral or slightly acidic medium (Yang et al., 2015; Chen et al., 2019).

At pH 7, the $H_2AsO_4^-$ / $HAsO_4^{2-}$ As(V) arsenic species are expected to be present in the reaction medium (Kumar et al., 2019), and according to pKa value for R-SH in L-Cys (~ 8.5), the thiol group is mostly protonated (Poole, 2015). Therefore, it is likely that the following reaction will take place:

$$2H^+ + HAsO_4^{2-} + 5R\text{-}SH \rightarrow As(SR)_3 + R\text{-}S\text{-}S\text{-}R + 4H_2O \quad (1)$$

In this reaction, the hydroxyl group (-OH) in arsenic species is displaced by thiol groups (R-SH, in the end-side of bounded L-Cys where R is $-CH_2CH(NH_2)COO\text{-}[CH\text{-}CH_2]_n$) in L-Cysteine, to yield the thiolate complexes (Carrero et al., 2001).

At low pH (pH < 5), arsenic adsorption likely occurs through electrostatic attraction between protonated amino groups (NH_3^+) in L-Cys and the negatively charged arsenic species. For example, it has been reported that negatively charged arsenic species can be adsorbed onto the positively charged surface of a chitosan-based membrane (Min et al., 2019). Besides, in the removal of chromium species by L-Cys-capped Fe_3O_4 nano-adsorbent, the main adsorption mechanism is the interaction of electronically rich anionic $HCrO_4^-$ species with a protonated amine at acid conditions (pH < 5) (Bashir et al., 2021). At pH > 8, the decrease in arsenic removal probably is due to the repulsive interaction between $HAsO_4^{2-}$ and the negatively charged surface of the adsorbent.

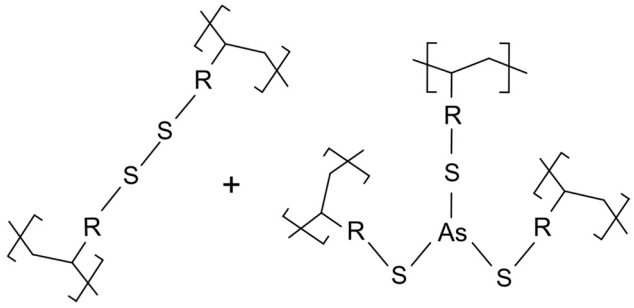

Fig. 9 – Reaction products of the proposed mechanism of arsenic bonding to PVA-LCys membrane, preceded by a reduction of As(V) to As(III), yielding a disulfide bond. R is $-CH_2CH(NH_2)COO\text{-}[CH\text{-}CH_2]_n$).

From these results, we can conclude that the dependency of arsenic removal on the pH of the medium suggests two modes of interaction of L-Cys with pentavalent arsenic. Thiolate complex formation through the -SH group at near-neutral pH is the primary mechanism for arsenic sorption. In contrast, at water pH values lower than 4, the interaction between protonated amino groups and anionic arsenic species predominates. Hence, the arsenic removal by L-Cys containing membrane is a pH-dependent process. Fig. 9 shows the As adsorption structure and the disulfide by-product based on the proposed reaction (Eq. 1).

3.6.2. *Adsorption kinetics and isotherm*

Testing adsorption kinetics is fundamental to understanding arsenic migration into the nanofibers.

Fig. 10 shows the adsorption kinetic curve of PVA-LCys 10% HT, varying the contact time up to 60 h. Fast initial adsorption is observed, with a characteristic time of 120 min and a slow convergence towards a stationary state at 480 min. To evaluate possible adsorption mechanisms, pseudo first order (PFO), pseudo second order (PSO), and Webber-Morris adsorption models were proposed. Among all of them, PFO best fits the kinetic results.

Pseudo first order kinetics is obtained from the differential equation $dq/dt = k\,(q_m - q)$, and can be expressed in its integral form as:

$$q(t) = q_m\,[1 - \exp(-k\,t)] \quad (2)$$

where q_m is the equilibrium adsorption capacity and k is the inverse of the characteristic time (Lagergreen, 1907). Its linearized form can be written as:

$$\ln(q_m - q(t)) = \ln(q_m) - k\,t \quad (3)$$

where it can be seen that q_m must be proposed as an input parameter. Given that this should be made by the trial-and-error method to obtain the optimal q_m value (Ho and McKay, 1998), a non-linear fitting was performed instead, as suggested by Tran et al. (2017). Kinetic of adsorption of the pseudo second order equation is obtained from equation $dq/dt = k_2\,(q_m - q)^2$, where k_2 is a constant and which integral

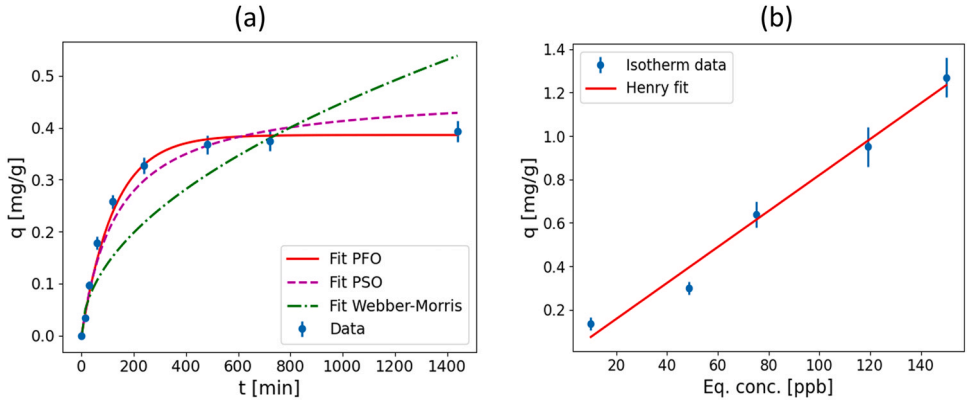

Fig. 10 – Adsorption kinetics (a) and adsorption isotherm (b) of PVA-LCys 10% HT, measured with a dose of 667 mg L-Cys/L and at pH 6.8.

form can be written as follows, in its non-linear form:

$$q(t) = q_m^2\, t / (1 / k + q_m / t) \quad (4)$$

Weber-Morris adsorption can be expressed as:

$$q(t) = k\, t^{0.5} + C \quad (5)$$

The goodness of fit was assessed with the reduced chi-squared statistic (χ^2_{red}), which is more suitable when comparing non-linear models and is encouraged to use in adsorption kinetic analysis (Tran et al., 2017). Table S2 (in SI) shows the summarized result of the tested models, from which we conclude that PFO better describes the chemical mechanism of adsorption. This fact can also be appreciated in the residual plots of the fits (Fig. S1).

Even though PFO is usually associated with physisorption in particulate sorbents (Alkurdi et al., 2021), the case presented in this work involves an encapsulated adsorbent inside highly hydrophilic nanofibers. Plazinski (2010) has shown that modeling adsorption kinetics using film diffusion mechanisms lead to PFO equation for the case of a Henry-like adsorption regime, even when chemisorption occurs in the core of the solid phase. We measured the adsorption isotherm of PVA-LCys 10% HT membrane to confirm this, shown in Fig. 10 (b). It is clearly observed that the isotherm of adsorption has a linear behavior ($R^2 = 0.98$), as expected from Henry's law. The equilibrium concentration range of the isotherm includes the one obtained in the kinetic adsorption experiment. With these results, we conclude that PFO is compatible with the diffusion of arsenate species into the nanofibers being the rate-controlling step. This means that arsenic must first enter the polymeric matrix, where species diffusion is slow as a consequence of tortuosity induced by the polymer, and then react with L-Cys to form the thiolate complex. This agrees with the usual adsorption mechanism of heavy metals in nanofibrous membranes (Talukder et al., 2021; Zhu et al., 2021).

Adsorption studies have shown that binding sites for arsenic species are readily accessible even when the adsorbent lies within the nanofibers, which is possible thanks to the hydrophilic nature of PVA and its capability to swell underwater (Cimadoro and Goyanes, 2020).

4. Conclusions

A bio-inspired membrane using a biodegradable polymer was successfully developed based on the immobilization of L-Cys inside PVA nanofibers. It can efficiently remove arsenic from water down to 10 µg/L, surpassing the adsorption performance of L-Cys found in the literature and without needing a further filtration process to remove the adsorbent.

Our results showed that L-Cys anchor covalently to PVA chains during heat treatment, providing active sites for arsenic adsorption in an insoluble, esterified/crosslinked structure. FTIR and TGA results demonstrate that L-Cys molecules are not released into the environment, even when washing the sample with water.

The maximum As(V) removal efficiency is obtained at neutral pH, the optimal for drinking water treatment. We have shown that thiolates are the leading functional groups responsible for arsenic binding to L-Cys. Adsorption kinetics could be modeled using the pseudo first order equation, compatible with subsurface diffusion of arsenic being rate-limiting in the adsorption process.

Given that the demand for new green solutions to remove arsenic from water increases continuously worldwide, these findings are a mainstay for developing electrospun PVA-based advanced nanostructured materials and bio-inspired composites for water filtration.

Declaration of Competing Interest

The authors declare that they have no known competing financial interests or personal relationships that could have appeared to influence the work reported in this paper.

Acknowledgments

We kindly acknowledge the financial support of University of Buenos Aires-UBA (UBACYT 2018–2020 N°20020170100381BA), ANPCyT (PICT 2017-2362), MINCyT ("Programa Ciencia y Tecnología Contra el Hambre" IF-2021-4378615-APN-SSCI#MCT), Consejo Superior de Investigacion Cientificas (CSIC), Spain (I-COOP+ 2020 COOPB20502), the Ministerio de Ciencia, Innovación y Universidades code PID2019-104650GB-C21 (MCIU/AEI/FEDER, UE) and IT1566-22 (Basque Government).

Appendix A. Supporting information

Supplementary data associated with this article can be found in the online version at doi:10.1016/j.cherd.2022.06.042.

References

Alkurdi, S.S.A., Al-Juboori, R.A., Bundschuh, J., Bowtell, L., Marchuk, A., 2021. Inorganic arsenic species removal from water using bone char: a detailed study on adsorption kinetic and isotherm models using error functions analysis. J. Hazard. Mater. 405, 124112. https://doi.org/10.1016/J.JHAZMAT.2020.124112

Arvand, M., Sayyar Ardaki, M., 2017. Poly-l-cysteine/electrospun copper oxide nanofibers-zinc oxide nanoparticles nanocomposite as sensing element of an electrochemical sensor for simultaneous determination of adenine and guanine in biological samples and evaluation of damage to dsDNA and DNA purine bases by UV radiation. Anal. Chim. Acta 986, 25–41. https://doi.org/10.1016/J.ACA.2017.07.057

Bahmani, P., Maleki, A., Daraei, H., Rezaee, R., Khamforoush, M., Dehestani Athar, S., Gharibi, F., Ziaee, A.H., McKay, G., 2019. Application of modified electrospun nanofiber membranes with α-Fe2O3 nanoparticles in arsenate removal from aqueous media. Environ. Sci. Pollut. Res. 26, 21993–22009. https://doi.org/10.1007/s11356-019-05228-5

Baigorria, E., Cano, L.A., Sanchez, L.M., Alvarez, V.A., Ollier, R.P., 2020. Bentonite-composite polyvinyl alcohol/alginate hydrogel beads: preparation, characterization and their use as arsenic removal devices. Environ. Nanotechnol. Monit. Manag. 14, 100364. https://doi.org/10.1016/J.ENMM.2020.100364

Bardach, A.E., Ciapponi, A., Soto, N., Chaparro, M.R., Calderon, M., Briatore, A., Cadoppi, N., Tassara, R., Litter, M.I., 2015. Epidemiology of chronic disease related to arsenic in Argentina: a systematic review. Sci. Total Environ. 538, 802–816. https://doi.org/10.1016/j.scitotenv.2015.08.070

Bashir, A., Pandith, A.H., Malik, L.A., Qureashi, A., Ganaie, F.A., Dar, G.N., 2021. Magnetically recyclable L-cysteine capped Fe3O4 nanoadsorbent: a promising pH guided removal of Pb (II), Zn(II) and HCrO4- contaminants. J. Environ. Chem. Eng. 9, 105880. https://doi.org/10.1016/J.JECE.2021.105880

Carrero, P., Malavé, A., Burguera, J.L., Burguera, M., Rondón, C., 2001. Determination of various arsenic species by flow injection hydride generation atomic absorption spectrometry: investigation of the effects of the acid concentration of different reaction media on the generation of arsines. Anal. Chim. Acta 438, 195–204. https://doi.org/10.1016/S0003-2670(01)00796-6

Chen, H., Sharma, S.K., Sharma, P.R., Yeh, H., Johnson, K., Hsiao, B.S., 2019. Arsenic(III) removal by nanostructured dialdehyde cellulose-cysteine microscale and nanoscale fibers. ACS Omega 4, 22008–22020. https://doi.org/10.1021/acsomega.9b03078

Cimadoro, J., Goyanes, S., 2020. Reversible swelling as a strategy in the development of smart membranes from electrospun polyvinyl alcohol nanofiber mats. J. Polym. Sci. 58, 737–746. https://doi.org/10.1002/pol.20190156

CONICET Argentina, 2018. Informe arsénico en agua. Red de Seguridad alimentaria-Consejo Nacional de Investigaciones Cientificas y Tecnicas. https://rsa.conicet.gov.ar/wp-content/uploads/2018/08/Informe-Arsenico-en-agua-RSA.pdf (accessed 18 june 2021).

de Dicastillo, C.L., Garrido, L., Alvarado, N., Romero, J., Palma, J.L., Galotto, M.J., 2017. Improvement of Polylactide Properties through Cellulose Nanocrystals Embedded in Poly(Vinyl Alcohol) Electrospun Nanofibers. Nanomater. 2017, Vol. 7, Page 106 7, 106. https://doi.org/10.3390/NANO7050106.

Dhar, R.K., Zheng, Y., Rubenstone, J., Van Geen, A., 2004. A rapid colorimetric method for measuring arsenic concentrations in groundwater. Anal. Chim. Acta 526, 203–209. https://doi.org/10.1016/J.ACA.2004.09.045

Estevez-Areco, S., Guz, L., Candal, R., Goyanes, S., 2018. Release kinetics of rosemary (Rosmarinus officinalis) polyphenols from polyvinyl alcohol (PVA) electrospun nanofibers in several food simulants. Food Packag. Shelf Life 18, 42–50. https://doi.org/10.1016/j.fpsl.2018.08.006

Giri, D.D., Jha, J.M., Tiwari, A.K., Srivastava, N., Hashem, A., Alqarawi, A.A., Abd_Allah, E.F., Pal, D.B., 2021. Java plum and amaltash seed biomass based bio-adsorbents for synthetic wastewater treatment. Environ. Pollut. 280, 116890. https://doi.org/10.1016/J.ENVPOL.2021.116890

Gonçalves, I.S., Costa, J.A.V., Morais, M.G. de, 2022. Microfiltration membranes developed from nanofibers via an electrospinning process. Mater. Chem. Phys. 277, 125509. https://doi.org/10.1016/J.MATCHEMPHYS.2021.125509

Guo, Q., Li, Y., Wei, X.Y., Zheng, L.W., Li, Z.Q., Zhang, K.G., Yuan, C.G., 2021. Electrospun metal-organic frameworks hybrid nanofiber membrane for efficient removal of As(III) and As(V) from water. Ecotoxicol. Environ. Saf. 228, 112990. https://doi.org/10.1016/J.ECOENV.2021.112990

Halicka, K., Cabaj, J., 2021. Electrospun nanofibers for sensing and biosensing applications—a review. Int. J. Mol. Sci. 2021 22, 6357. https://doi.org/10.3390/IJMS22126357

Ho, Y.S., McKay, G., 1998. A comparison of chemisorption kinetic models applied to pollutant removal on various sorbents. Process Saf. Environ. Prot. 76, 332–340. https://doi.org/10.1205/095758298529696

Holland, B.J., Hay, J.N., 2001. The thermal degradation of poly (vinyl alcohol). Polymer 42, 6775–6783. https://doi.org/10.1016/S0032-3861(01)00166-5

Kogelheide, F., Kartaschew, K., Strack, M., Baldus, S., Metzler-Nolte, N., Havenith, M., Awakowicz, P., Stapelmann, K., Lackmann, J.W., 2016. FTIR spectroscopy of cysteine as a ready-to-use method for the investigation of plasma-induced chemical modifications of macromolecules. J. Phys. D Appl. Phys. 49, 084004. https://doi.org/10.1088/0022-3727/49/8/084004

Koski, A., Yim, K., Shivkumar, S., 2004. Effect of molecular weight on fibrous PVA produced by electrospinning. Mater. Lett. 58, 493–497. https://doi.org/10.1016/S0167-577X(03)00532-9

Kumar, R., Patel, M., Singh, P., Bundschuh, J., Pittman, C.U., Trakal, L., Mohan, D., 2019. Emerging technologies for arsenic removal from drinking water in rural and peri-urban areas: methods, experience from, and options for Latin America. Sci. Total Environ. 694, 133427. https://doi.org/10.1016/J.SCITOTENV.2019.07.233

Lagergreen, S., 1907. Zur Theorie der sogenannten Adsorption gelöster Stoffe - (Bihang A. K. Svenske Vet. Ak. Handl. 24, II. Nr. 4, S. 49; 1899; Z. physik. Ch. 32, 174–75; 1900.) Zeitschrift für Chemie und Ind. der Kolloide 2, 15. https://doi.org/10.1007/BF01501332.

Lim, L.Y., Wan, L.S.C., 2008. The Effect of Plasticizers on the Properties of Polyvinyl Alcohol Films. http://dx.doi.org/10.3109/03639049409038347 20, 1007–1020.

Litter, M.I., Ingallinella, A.M., Olmos, V., Savio, M., Difeo, G., Botto, L., Torres, E.M.F., Taylor, S., Frangie, S., Herkovits, J., Schalamuk, I., González, M.J., Berardozzi, E., García Einschlag, F.S., Bhattacharya, P., Ahmad, A., 2019. Arsenic in Argentina: technologies for arsenic removal from groundwater sources, investment costs and waste management practices. Sci. Total Environ. 690, 778–789. https://doi.org/10.1016/j.scitotenv.2019.06.358

Liu, Y., Wang, R., Ma, H., Hsiao, B.S., Chu, B., 2013. High-flux microfiltration filters based on electrospun polyvinylalcohol nanofibrous membranes. Polymer 54, 548–556. https://doi.org/10.1016/J.POLYMER.2012.11.064

López-Córdoba, A., Castro, G.R., Goyanes, S., 2016. A simple green route to obtain poly(vinyl alcohol) electrospun mats with improved water stability for use as potential carriers of drugs. Mater. Sci. Eng. C 69, 726–732. https://doi.org/10.1016/j.msec.2016.07.058

Makavipour, F., Pashley, R.M., Rahman, A.F.M.M., 2019. Low-level arsenic removal from drinking water. Glob. Chall. 3, 1700047. https://doi.org/10.1002/gch2.201700047

Min, L.-L., Yang, L.-M., Wu, R.-X., Zhong, L.-B., Yuan, Z.-H., Zheng, Y.-M., 2019. Enhanced adsorption of arsenite from aqueous solution by an iron-doped electrospun chitosan nanofiber mat: preparation, characterization and performance. J. Colloid Interface Sci. 535, 255–264. https://doi.org/10.1016/J.JCIS.2018.09.073

Min, L.L., Yuan, Z.H., Zhong, L., Bin, Liu, Q., Wu, R.X., Zheng, Y.M., 2015. Preparation of chitosan based electrospun nanofiber

membrane and its adsorptive removal of arsenate from aqueous solution. Chem. Eng. J. 267, 132–141. https://doi.org/10.1016/J.CEJ.2014.12.024

Miraftab, M., Saifullah, A.N., Çay, A., 2015. Physical stabilisation of electrospun poly(vinyl alcohol) nanofibres: comparative study on methanol and heat-based crosslinking. J. Mater. Sci. 50, 1943–1957. https://doi.org/10.1007/s10853-014-8759-1

Mohammed Abdul, K.S., Jayasinghe, S.S., Chandana, E.P.S., Jayasumana, C., De Silva, P.M.C.S., 2015. Arsenic and human health effects: a review. Environ. Toxicol. Pharmacol. 40, 828–846. https://doi.org/10.1016/J.ETAP.2015.09.016

Negrea, A., Popa, A., Ciopec, M., Lupa, L., Negrea, P., Davidescu, C.M., Motoc, M., Mînzatu, V., 2014. Phosphonium grafted styrene-divinylbenzene resins impregnated with iron(III) and crown ethers for arsenic removal. Pure and Applied Chemistry. Walter de Gruyter GmbH, pp. 1729–1740. https://doi.org/10.1515/pac-2014-0806

Oliveira, V.H.B., Rechotnek, F., da Silva, E.P., Marques, V., de, S., Rubira, A.F., Silva, R., Lourenço, S.A., Muniz, E.C., 2020. A sensitive electrochemical sensor for Pb^{2+} ions based on ZnO nanofibers functionalized by L-cysteine. J. Mol. Liq. 309, 113041. https://doi.org/10.1016/j.molliq.2020.113041

Pereira, F.J., Vázquez, M.D., Debán, L., Aller, A.J., 2014. Spectrometric characterisation of the solid complexes formed in the interaction of cysteine with As(III), Th(IV) and Zr(IV). Polyhedron 76, 71–80. https://doi.org/10.1016/J.POLY.2014.03.036

Pereira, P.P., Fernandez, M., Cimadoro, J., González, P.S., Morales, G.M., Goyanes, S., Agostini, E., 2021. Biohybrid membranes for effective bacterial vehiculation and simultaneous removal of hexavalent chromium (CrVI) and phenol. Appl. Microbiol. Biotechnol. 105, 827–838. https://doi.org/10.1007/s00253-020-11031-x

Plazinski, W., 2010. Applicability of the film-diffusion model for description of the adsorption kinetics at the solid/solution interfaces. Appl. Surf. Sci. 256, 5157–5163. https://doi.org/10.1016/J.APSUSC.2009.12.083

Poole, L.B., 2015. The basics of thiols and cysteines in redox biology and chemistry. Free Radic. Biol. Med. 80, 148–157. https://doi.org/10.1016/j.freeradbiomed.2014.11.013

Ray, S.S., Chen, S.S., Li, C.W., Nguyen, N.C., Nguyen, H.T., 2016. A comprehensive review: Electrospinning technique for fabrication and surface modification of membranes for water treatment application. RSC Adv. 6, 85495–85514. https://doi.org/10.1039/c6ra14952a

Ribba, L., Cimadoro, J., D'Accorso, N., Goyanes, S., 2017. Removal of pollutants using electrospun nanofiber membranes. Industrial Applications of Renewable Biomass Products: Past, Present and Future. pp. 301–324. https://doi.org/10.1007/978-3-319-61288-1_12

Shen, S., Li, X.F., Cullen, W.R., Weinfeld, M., Le, X.C., 2013. Arsenic binding to proteins. Chem. Rev. 113, 7769–7792. https://doi.org/10.1021/cr300015c

Socrates, G., 2004. Infrared and Raman Characteristic Group Frequencies, Third Edit. John Wiley & Sons, New York. https://doi.org/10.1002/jrs.1238

Solangi, N.H., Kumar, J., Mazari, S.A., Ahmed, S., Fatima, N., Mubarak, N.M., 2021. Development of fruit waste derived bio-adpsorbents for wastewater treatment: a review. J. Hazard. Mater. 416, 125848. https://doi.org/10.1016/J.JHAZMAT.2021.125848

Sonker, A.K., Rathore, K., Nagarale, R.K., Verma, V., 2018. Crosslinking of polyvinyl alcohol (PVA) and effect of crosslinker shape (aliphatic and aromatic) thereof. J. Polym. Environ. 26, 1782–1794. https://doi.org/10.1007/s10924-017-1077-3

Spuches, A.M., Kruszyna, H.G., Rich, A.M., Wilcox, D.E., 2005. Thermodynamics of the as(III)-thiol interaction: arsenite and monomethylarsenite complexes with glutathione, dihydrolipoic acid, and other thiol ligands. Inorg. Chem. 44, 2964–2972. https://doi.org/10.1021/ic048694q

Srithep, Y., Pholharn, D., 2017. Plasticizer effect on melt blending of polylactide stereocomplex. E-Polymers 17, 409–416. https://doi.org/10.1515/epoly-2016-0331

Talukder, M.E., Pervez, M.N., Jianming, W., Gao, Z., Stylios, G.K., Hassan, M.M., Song, H., Naddeo, V., 2021. Chitosan-functionalized sodium alginate-based electrospun nanofiber membrane for As (III) removal from aqueous solution. J. Environ. Chem. Eng. 9, 106693. https://doi.org/10.1016/J.JECE.2021.106693

Tam, L.M., Price, N.E., Wang, Y., 2020. Molecular mechanisms of arsenic-induced disruption of DNA repair. Chem. Res. Toxicol. https://doi.org/10.1021/acs.chemrestox.9b00464

Taylor, S. 2017. Arsénico en las Aguas Subterráneas en Buenos Aires. Mapa de Situación. Autoridad del Agua (ADA).

Tian, H., Yuan, L., Wang, J., Wu, H., Wang, H., Xiang, A., Ashok, B., Rajulu, A.V., 2019. Electrospinning of polyvinyl alcohol into crosslinked nanofibers: an approach to fabricate functional adsorbent for heavy metals. J. Hazard. Mater. 378, 120751. https://doi.org/10.1016/j.jhazmat.2019.120751

Timalsina, H., Mainali, B., Angove, M.J., Komai, T., Paudel, S.R., 2021. Potential modification of groundwater arsenic removal filter commonly used in Nepal: a review. Groundw. Sustain. Dev. 12, 100549. https://doi.org/10.1016/J.GSD.2021.100549

Torasso, N., Vergara-Rubio, A., Rivas-Rojas, P., Huck-Iriart, C., Larrañaga, A., Fernández-Cirelli, A., Cerveny, S., Goyanes, S., 2020. Enhancing arsenic adsorption via excellent dispersion of iron oxide nanoparticles inside poly(vinyl alcohol) nanofibers. J. Environ. Chem. Eng. 9, 104664. https://doi.org/10.1016/j.jece.2020.104664

Tran, H.N., You, S.J., Hosseini-Bandegharaei, A., Chao, H.P., 2017. Mistakes and inconsistencies regarding adsorption of contaminants from aqueous solutions: a critical review. Water Res. https://doi.org/10.1016/j.watres.2017.04.014

Tripathy, M., Padhiari, S., Hota, G., 2020. L-Cysteine-functionalized mesoporous magnetite nanospheres: synthesis and adsorptive application toward arsenic remediation. J. Chem. Eng. Data 65, 3906–3919. https://doi.org/10.1021/acs.jced.0c00250

Vergara-Rubio, A., Ribba, L., Picón, D., Candal, R., Goyanes, S., 2022. A highly efficient nanostructured sorbent of sulfuric acid from ecofriendly electrospun poly(vinyl alcohol) mats. Ind. Eng. Chem. Res. 61, 2091–2099. https://doi.org/10.1021/acs.iecr.1c03530

World Health Organization (WHO) Switzerland, 2017. Guidelines for Drinking-water Quality. 4th ed., ⟨https://www.who.int/publications/i/item/9789240045064⟩ (accessed 18 june 2021).

Yang, R., Su, Y., Aubrecht, K.B., Wang, X., Ma, H., Grubbs, R.B., Hsiao, B.S., Chu, B., 2015. Thiol-functionalized chitin nanofibers for As (III) adsorption. Polymer 60, 9–17. https://doi.org/10.1016/J.POLYMER.2015.01.025

Zhang, Y., Wang, F., Wang, Y., 2021. Recent developments of electrospun nanofibrous materials as novel adsorbents for water treatment. Mater. Today Commun. 27, 102272. https://doi.org/10.1016/J.MTCOMM.2021.102272

Zhu, F., Zheng, Y.M., Zhang, B.G., Dai, Y.R., 2021. A critical review on the electrospun nanofibrous membranes for the adsorption of heavy metals in water treatment. J. Hazard. Mater. 401, 123608. https://doi.org/10.1016/J.JHAZMAT.2020.123608